Article

Redox-Sensitive Citronellol-Cabazitaxel Conjugate: Maintained in Vitro Cytotoxicity and Self-Assembled as Multifunctional Nanomedicine

Peng Xue, Dan Liu, Jing Wang, Na Zhang, Jiahua Zhou, Lin Li, Weiling Guo, Mengchi Sun, Xiangfei Han, and Yongjun Wang

Bioconjugate Chem., **Just Accepted Manuscript** • DOI: 10.1021/acs.bioconjchem.6b00155 • Publication Date (Web): 12 Apr 2016

Redox-Sensitive Citronellol-Cabazitaxel Conjugate: Maintained *in Vitro* Cytotoxicity and Self-Assembled as Multifunctional Nanomedicine

Peng Xue,[†] Dan Liu,[‡] Jing Wang,[†] Na Zhang,[‡] Jiahua Zhou,[†] Lin Li,[†] Weiling Guo,[†] Mengchi Sun,[†] Xiangfei Han,[†] and Yongjun Wang*[,†]

[†] *School of Pharmacy, Shenyang Pharmaceutical University, No. 103, Wenhua Road, Shenyang, 110016, China*

[‡] *Key Laboratory of Structure-Based Drug Design and Discovery, Ministry of Education, Shenyang Pharmaceutical University, No. 103, Wenhua Road, Shenyang, 110016, China*

ABSTRACT GRAPHIC

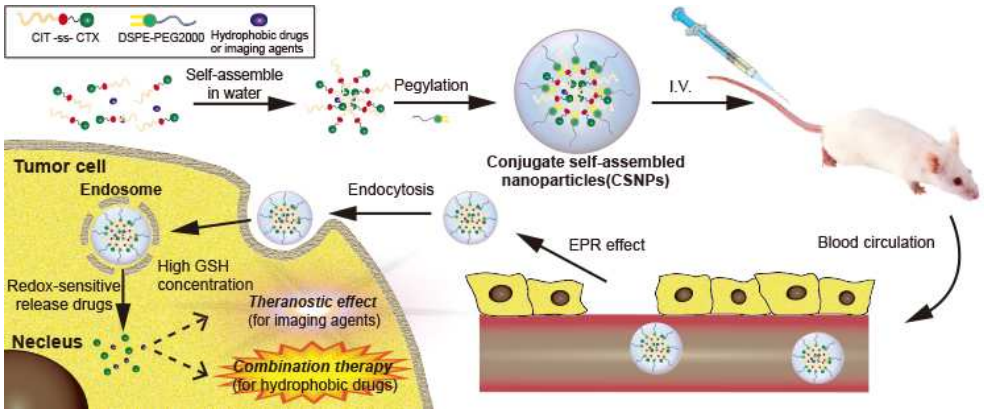

ABSTRACT

Citronellol-cabazitaxel (CIT-ss-CTX) conjugate self-assembled nanoparticles (CSNPs) were designed and prepared by conjugating cabazitaxel with citronellol via the disulfide bond that is redox-sensitive to the high concentration of glutathione within tumor cells. Notably, the CSNPs maintained in the cell cytotoxicity. Moreover, the AUC_{0-t} of CSNPs was 6.5-fold higher than that of cabazitaxel solutions and the $t_{1/2}$ was prolonged 2.3 times. Furthermore, we found that CSNPs could be employed as an efficient carrier for other hydrophobic drugs or imaging agents. Thus the *in vivo* targeting study was implemented via using 1,1-dioctadecyl-3,3,3,3-tetramethylindotricarbocyanine iodide (DiR)-loaded CSNPs as imaging agent, which showed CSNPs could effectively accumulate at tumor site. And curcumin, a hydrophobic anticancer drug, was successfully loaded in CSNPs which exhibits good stability and synergistic antitumor effects. The citronellol-cabazitaxel conjugate therefore has a promising perspective as a multifunctional nanomedicine for combination therapy and theranostics attribute to its long circulation property, redox-sensitive mechanism and high drug co-loading capability.

KEYWORDS: cabazitaxel, disulfide bond, conjugate self-assembled nanoparticles, redox-sensitive, multifunctional nanomedicine

INTRODUCTION

Cabazitaxel (CTX) is an anticancer drug of taxanes which can be used for the treatment of metastatic castration-resistant prostate cancer (mCRPC).[1,2] It has the similar mechanism with docetaxel that act by binding to microtubules, thereby promoting the assembly of tubulin into stable microtubules and simultaneously inhibiting disassembly, which results in the blockage of mitosis at the G2/M phase and leads to cell death.[3,4] Cabazitaxel (Jevtana, Sanofi–Aventis) was approved by the US Food and Drug Administration (FDA) in June 2010.[5] Jevtana used in clinic requires two times of dilutions before intravenous infusion, and it has a significant advantage that can overcome multidrug resistance (MDR) due to its poor affinity to P-glycoprotein (P-gp) — a member of the MDR protein family that pumps the intracellular drug out of cells — compared with docetaxel and paclitaxel.[6] But there also exists some problems: the drug solutions must be prepared immediately before use because of the instability of cabazitaxel and it has adverse side effects especially to neutropenia and leucopenia.[7] In the past years, biocompatible nanosystems such as polymeric micelles and polymeric nanoparticles have been designed for the delivery of cabazitaxel[8-12] and have improved safety and the ability of targeting tumor site due to the enhanced permeability and retention (EPR) effect.[13] Nevertheless, the nanosystems suffer low drug loading capacity and poor stability *in vivo*. An appropriate drug delivery system should be developed to improve the drug loading capacity and control the release of drug in tumor site.

Tumor microenvironment, referring to cellular components such as endothelial cells, tumor-associated macrophages, cancer-associated fibroblasts, inflammatory cells and non-cellular components such as matrix metalloproteinases, integrins, cytokines and their receptors, is suitable for tumor growth, invasion and metastasis.[14-

[16] These cellular and non-cellular components give tumor microenvironment special features including hypoxia, acidic, interstitial hypertension and chronic inflammatory response.[17] And the tumor intracellular microenvironment is quite particular because of its strong redox status caused by the high concentration of glutathione (GSH, 1-11 mM) compared with GSH in blood circulatory system (4-8 μM).[18,19] Thus, some studies have designed redox-sensitive drug delivery system such as redox-sensitive micelles for improving the targeting effect on tumor cells. These sensitive micelles usually contain disulfide linkage that is stable in blood circulation and can be rapidly cleaved through thiol-disulfide exchange reactions with tumor intracellular GSH.[19-21] In our previous study, the disulfide-linked prodrugs such as paclitaxel-ss-vetamin E were synthesized and used self-assembled into nanoparticles.[22] DSPE-PEG2000 was used as stabilizer which the hydrophobic part was inserted into the nanoparticles and the PEG chains were exposed to the surface to give the nanoparticles a feature of long circulation that the nanoparticles could not be recognized and cleared by the reticuloendothelial system.[16] The nanoparticles have good stability and GSH-triggered drug release, demonstrating that self-assembled nanoparticles can be employed for effective delivering drugs to tumor intracellular microenvironment.

Citronellol (CIT) is a monoterpene alcohol which has antioxidant and antiinflammatory properties.[23,24] It has been reported that citronellol has moderate anticancer activities, and it may sensitize the activities of other anticancer drugs.[25] It also was reported that citronellol could improve the immune function of cancer patients and their ability to fight off the cancer.[23] For these reasons, we synthesized the novel cabazitaxel prodrug by conjugating cabazitaxel with citronellol via disulfide bond. Then the conjugate self-assembled nanoparticles (CSNPs) were prepared and the physical and chemical properties of the CSNPs were characterized. *In vitro*, the

cell viability assay, cell uptake, cell cycle analysis and cell apoptosis on A549 cells and PC3 cells of the CSNPs were studied. *In vivo,* the pharmacokinetics and biodistribution of the CSNPs injected via tail vein were evaluated in rats. Furthermore, we put forward an innovative idea that CSNPs can be utilized as an effective carrier for other hydrophobic drugs or imaging agents. So fluorescence dyes 6-coumarin and 1,1-dioctadecyl-3,3,3,3-tetramethylindotricarbocyanine iodide (DiR) were chosen to prepare the 6-coumarin-loaded CSNPs and DiR-loaded CSNPs for the study of cell uptake and *in vivo* biodistribution of CSNPs, respectively. And curcumin with diverse effects including antiproliferative, anti-inflammatory, antiangiogenic and antioxidant activities[26-28] was selected as a model drug to load in CSNPs, then the stability and synergistic antitumor effects of curcumin-loaded CSNPs was investigated.

RESULTS AND DISCUSSION

Synthesis of Citronellol-cabazitaxel Conjugate. Cabazitaxel was conjugated with citronellol via disulfide bond (Scheme 1). Firstly, dithiodiglycolic acid (DTDA) was converted to the corresponding anhydride with acetic anhydride as dehydration agent. Then, it reacted with citronellol to obtain CIT-DTDA **w**ith 4-dimethylaminopyridine (DMAP) as catalyst. Finally, CIT-DTDA was reacted with cabazitaxel under 1-ethyl-3-(3-dimethyllaminopropyl)carbodiimide hydrochloride (EDCI), 1-Hydroxybenzotriazole (HOBt) and DMAP to gain the target compound citronellol-cabazitaxel conjugate (CIT-ss-CTX).

Scheme 1. Synthesis of citronellol-cabazitaxel conjugate[a]

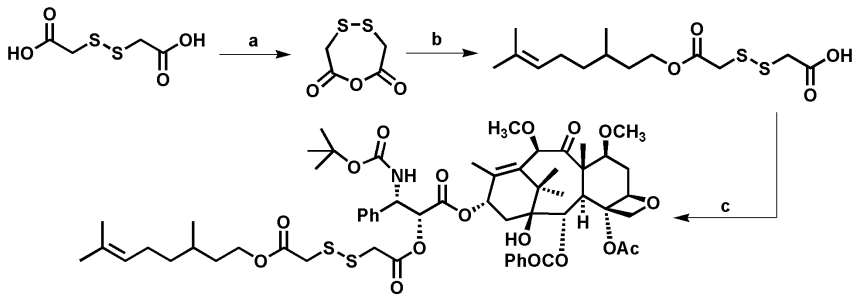

[a]Conditions : (a) Ac_2O, 25°C; (b) citronellol, DMAP, DCM, r.t.; (c) cabazitaxel, EDCI, HOBt, DMAP, DCM, 0-r.t.

The chemical structure of citronellol-cabazitaxel conjugate was confirmed by ^1H NMR (Figure 1). The ^1H NMR spectra of citronellol-cabazitaxel conjugate (400 MHz, $CDCl_3$) was analyzed as following: δ8.10 (2H, d, 3″7″), 7.61 (1H, m, 5″), 7.50 (2H, m, 4″6″), 7.40-7.34 (4H, m, 5′6′8′9′), 7.32 (1H, m, 7′), 6.24 (1H, t, H13), 5.64 (1H, d, H2), 5.49 (1H, br.s, H3′), 5.34 (1H, br.s, H2′), 5.08 (1H, t, $CH(CH_3)_2$=CH), 4.98 (1H, d, H5), 4.82 (1H, s, H10), 4.30(1H, d, H20), 4.18 (2H, m, -CO_2CH_2), 4.16 (1H, d, H20), 3.90 (1H, m, H7), 3.84 (1H, d, H3), 3.62 (2H, s, -SCH_2CO_2-CTX), 3.54 (2H, s, -SCH_2CO_2-CIT), 3.43 (3H, s, 10-OCH_3), 3.30 (3H, s, 7-OCH_3), 2.70 (1H, m, H6),

2.43 (3H, s, 4-$OCOCH_3$), 2.27 (1H, m, H14), 2.00 (2H, s, $=CHCH_2$-CH_2), 1.99 (3H, s, 18-CH_3), 1.79-1.75 (2H, m, H14, H6), 1.71 (3H, s, 19-CH_3), 1.68 (3H, s, $=CH(CH_3)_2$), 1.60 (3H, s, $=CH(CH_3)_2$), 1.55-1.48 (4H, m, $-OCH_2CH_2CH(CH_3)CH_2$), 1.35 (9H, s, $(OCH_3)_3$), 1.21 (3H, s, 16-CH_3), 1.19 (3H, s, 17-CH_3), 0.92 (3H, d, $-OCH_2CH(CH_3)$). ^{1}H NMR spectrum displayed new peaks at δ5.08/4.18/0.92 and δ3.62/3.54, which can be attributed to the protons of CIT and methylene protons of the disulfide linker, respectively. Furthermore, the chemical shift of H2' in CTX moved to the low field to 5.34, indicating that CIT-DTDA was successfully conjugated to CTX via an ester bond at C2'.

The final product was also characterized by Bruker micrOTOF-Q time of flight mass spectrometer which was a powerful method to detect the mass of the compound. The accurate m/z 1160.4682 ions was determined as sodium adduct ($[C_{59}H_{79}NO_{17}S_2+Na]^+$ ions) for citronellol-cabazitaxel conjugate (Figure 2). The predicted molecular formula is matched with actual molecular formula.

The results above indicated that cabazitaxel was successfully conjugated to citronellol via disulfide bond.

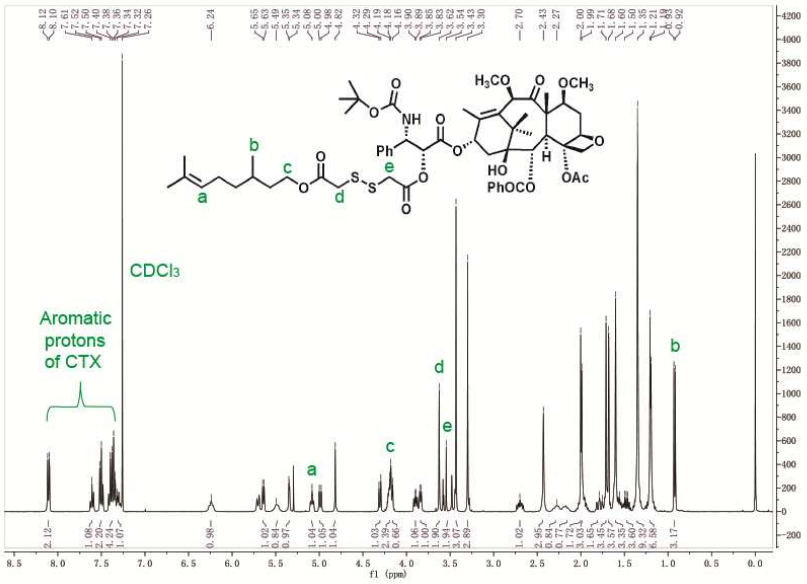

Figure 1. ^{1}H NMR spectra of citronellol-cabazitaxel conjugate (400 MHz, $CDCl_3$).

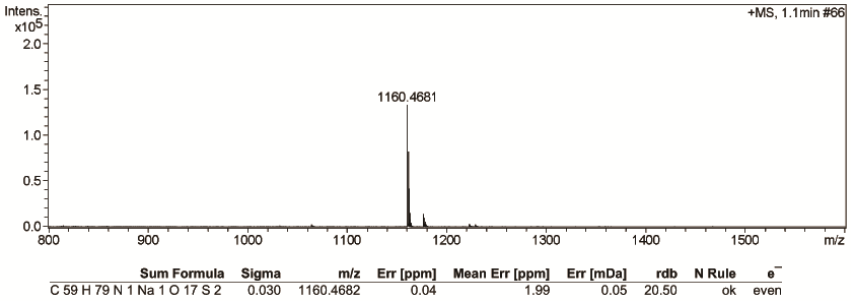

Sum Formula	Sigma	m/z	Err [ppm]	Mean Err [ppm]	Err [mDa]	rdb	N Rule	e⁻
C 59 H 79 N 1 Na 1 O 17 S 2	0.030	1160.4682	0.04	1.99	0.05	20.50	ok	even

Figure 2. MS spectra of citronellol-cabazitaxel conjugate.

Preparation and Characterization of CSNPs. It was found that self-assembled nanoparticles could be prepared by nano-precipitation method in our previous work.[22] In this study, the citronellol-cabazitaxel conjugate self-assembled nanoparticles were prepared by the same way. DLS analysis revealed that the CSNPs had a size of 153.3 ± 0.17 nm, PDI of 0.081 ± 0.009 and Zeta potential of -19.0 ± 2.55 mV (Table S1), suggesting that the CSNPs could accumulate abundantly by EPR effect because the particle size of the CSNPs was between the endothelial junctions of normal vessels (less than 10 nm) and the fenestrations of tumor vasculatures (more than 200 nm).[29] And TEM micrograph (Figure 3B) indicated that CSNPs were spherical and the particle size was nearly 150 nm that close to the results detected by DLS. The loading content of cabazitaxel was 61.21 wt%, which was significantly higher than other nanomedicine such as polymeric micelles,[30] liposomes,[31] nanoemulsions,[32] and nanoparticles for delivery of taxane drug.[33] In addition, the stability of CSNPs stored at 4 °C was detected by DLS for two months (Figure S1C). And there were no significant changes in size and PDI of CSNPs. The particle size only slightly increased in the initial days which might caused by the internal hydrophobic interaction and the PDI was always below 0.2, indicting that the CSNPs were stable during storage at 4 °C. All these results proved the successful formation of stable spherical CSNPs with monomodal particle size distribution and low polydispersities.

And we thought that electrostatic repulsion of the surface charge of nanoparticles and the feature of conjugate that inhibits crystallization made the main contribution to the stable self-assembly of citronellol-cabazitaxel conjugate (Figure S2).

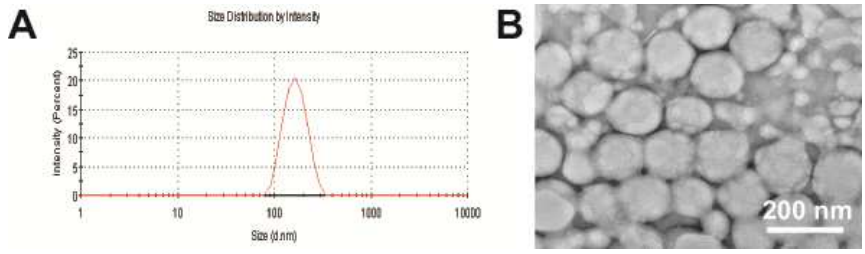

Figure 3. Size distribution of CSNPs determined by DLS (A) and TEM image of CSNPs (bar = 200 nm) (B).

***In Vitro* Drug Release Study.** The *in vitro* drug release of CSNPs was studied at 37 °C under four GSH conditions, including GSH 10 mM, 1 mM, 10 μM and, 1 μM respectively. The results showed that degradation of citronellol-cabazitaxel conjugate and the release of cabazitaxel were significantly accelerated under high concentration of GSH (Figure 4). For instance, 35.0%, 47.3%, 17.5%, 13.3% of cabazitaxel were released from the CSNPs and 98.5%, 89.4%, 73.9%, 72.8% of citronellol-cabazitaxel conjugate were degraded at 37 °C in 24h in PBS (pH 7.4) with 10 mM GSH, 1 mM GSH, 10 μM GSH and 1 μM GSH, respectively. The breakage of disulfide bond of citronellol-cabazitaxel conjugate caused by the high concentration of GSH can not directly generate cabazitaxel, it also need extra reaction to cleave the ester bond for the release of cabazitaxel which was a slow step. So the release rate of cabazitaxel was slow than the degradation rate of citronellol-cabazitaxel conjugate. And the release of cabazitaxel in the condition of 10 mM GSH was less than that of 1 mM GSH which might due to the slightly instability of cabazitaxel at high concentration of 10 mM GSH (Figure S3). Notably, we observed that the degradation rate of citronellol-cabazitaxel conjugate was: 10 mM GSH > 1 mM GSH > 10 μM GSH > 1 μM GSH. And it was obvious that the high concentration of GSH (1-10 mM)

corresponding to the intracellular GSH concentration in tumor cells[18, 19] could promote stronger cleavage of disulfide bonds of citronellol-cabazitaxel conjugate to release cabazitaxel (47.3% and 35.0%) compared with low concentration of GSH (1-10 μM) which was set as the redox condition in blood plasma(13.3% and 17.5%) in 24 h, which indicated that the CSNPs could reduce systemic toxicity by slow release of cabazitaxel at the blood circulation and rapid release within the tumor intracellular microenvironment.

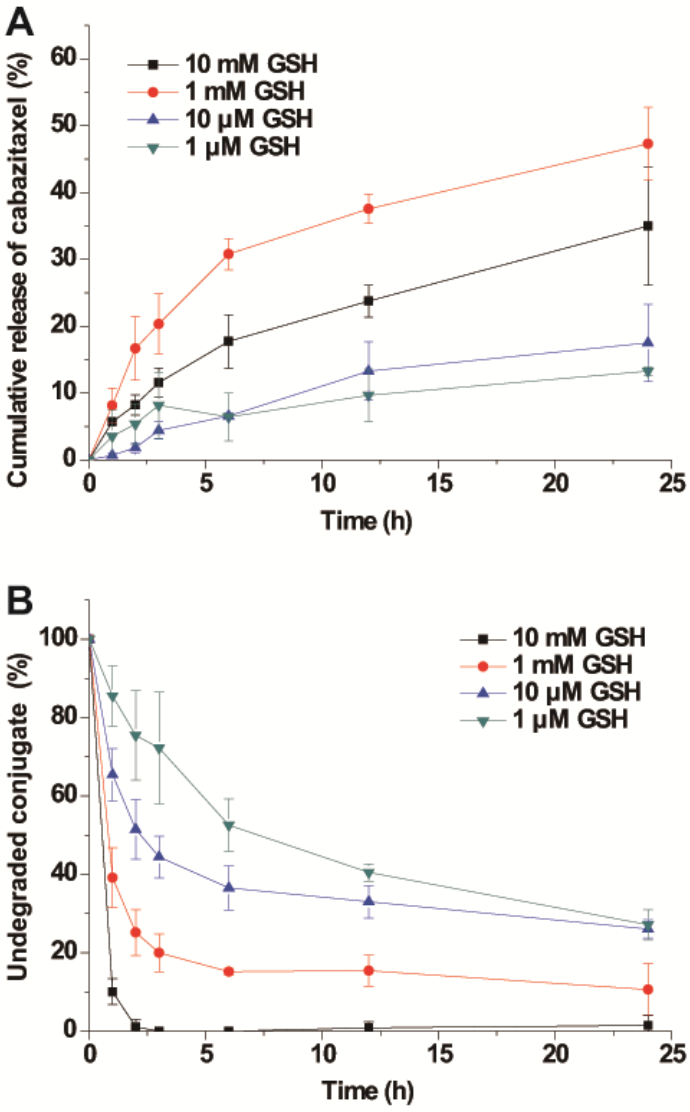

Figure 4. *In vitro* release studies. The GSH-sensitive release of cabazitaxel (A) and degradation of

citronellol-cabazitaxel conjugate (B) from CSNPs were studied at 37 °C under four different conditions, i.e, 10 mM, 1 mM, 10 μM and 1 μM GSH, respectively (n = 3).

Rat Plasma Stability. The addition of an esterase inhibitor is a usual method to stabilize compounds which can be hydrolyzed by esterase in serum, and phenylmethanesulfonyl fluoride (PMSF) has been tested and used as an inhibitor for esterase.[34-36] So the stability of CSNPs was studied at 37 °C in two media which were rat plasma containing 2.5 mM PMSF and without PMSF, respectively. As shown in Figure S4, although PMSF could stabilize the ester bonds in citronellol-cabazitaxel conjugate. The conjugate had the similar degraded behavior in two media, which suggested that the ester bonds have slightly influence on the degradation of conjugate. And we found that the degraded rate of conjugate in rat plasma just like that in PBS with 1~10μM GSH that revealed the GSH level in plasma (Figure 4B). This indicated that the major factor on the unstability of conjugate was the breakage of disulfide bond in terms of GSH. In addition, a reference about paclitaxel prodrug proved that the disulfide bond was cleaved through thiol-disulfide exchange reactions prior to the breakage of ester bonds in blood circulation.[37]

Cell Viability Assay. The *in vitro* antitumor activity of cabazitaxel solutions, CSNPs and citronellol solutions was investigated by MTT assays. Figure 5 showed that CSNPs maintained the cell cytotoxicity to both PC3 and A549 cells. Notably, CSNPs induced similar antitumor drug efficacy to cabazitaxel solutions in both PC3 and A549 cells. The IC_{50} of PC3 cells incubated with cabazitaxel solutions and CSNPs were 0.12 ± 0.01 nM and 0.70 ± 0.04 nM, respectively. And the IC_{50} of A549 cells incubated with cabazitaxel solutions and CSNPs were 4.26 ± 0.17 nM and 4.33 ± 0.27 nM, respectively (Table S2). Cabazitaxel solutions and CSNPs had almost the same antitumor activity on PC3 cells at various concentrations, however, antitumor activity of CSNPs became higher than cabazitaxel solutions on A549 cells at drug

concentrations less than 1 nM. Usually the cytotoxic activity of anticancer drug would decrease in dozens to hundreds of times after conjugation,[38,39] so it is noteworthy that the cytotoxic activity of CSNPs keeps almost unchanged. The similar antitumor activity of CSNPs and cabazitaxel solutions might be due to their fast drug release within cells resulting from the redox-responsive characteristic of citronellol-cabazitaxel conjugate, as well as the potential anticancer sensitizing effect of citronellol to cabazitaxel (Figure S5). The cell inhibition rate (%) of PC3 cells incubated with citronellol solutions was less than 15% at concentrations varying from 0.001 nM to 10 nM, suggesting that free citronellol had little antitumor effect to PC3 cells, but citronellol solutions had no antitumor effect to A549 cells.

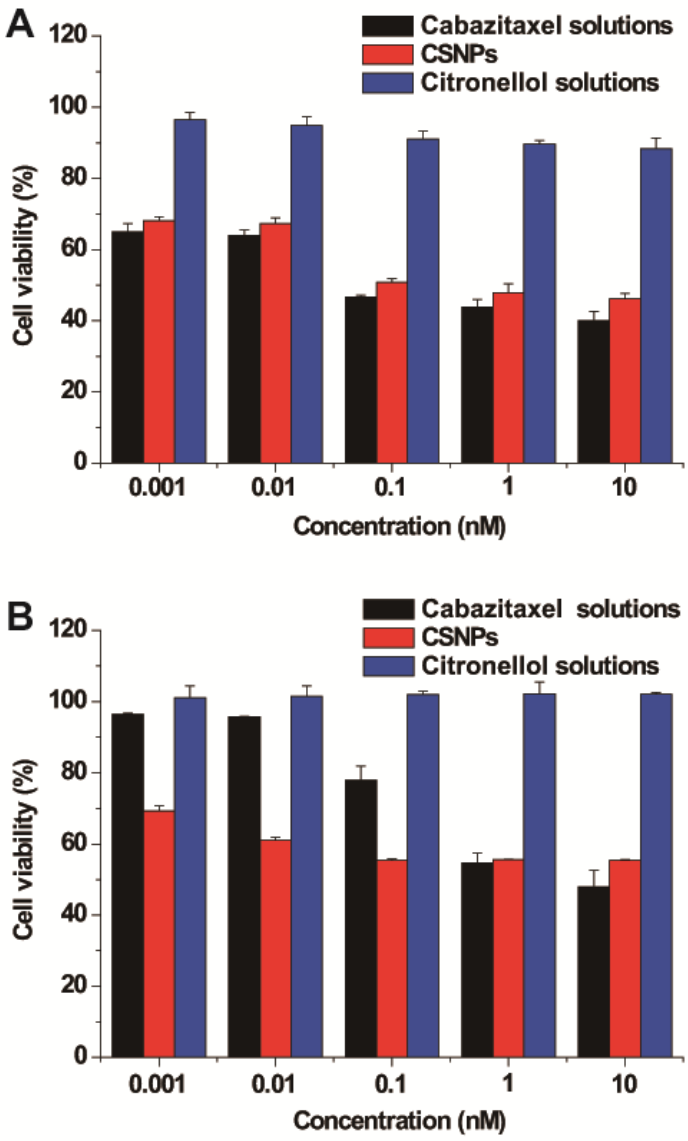

Figure 5. MTT assays of cabazitaxel solutions, CSNPs and citronellol solutions on PC3 cells (A) and A549 cells (B). The cells were incubated with formulations for 48 h at concentrations varying from 0.001 nM to 10 nM. Data are presented as mean ± SD (n = 3).

Cell Uptake Study. CSNPs had no fluorescence signal, hence we attempted to prepare the coumarin-6 loaded CSNPs to investigate the cell uptake of CSNPs in PC3 and A549 cells. The coumarin-6 loaded CSNPs were successfully prepared with light yellow green opalescence (Figure S6). And the weight of citronellol-cabazitaxel conjugate was 10 times of that of coumarin-6 and the cells were treated with

formulations for only 1 h and 3 h, so the effect of citronellol-cabazitaxel conjugate on cells could be ignored.

The CLSM images were presented in Figure 6. It clearly showed that compared with the treatment with CSNPs loaded 1 μg/mL coumarin-6 for 1 h, the cells treated with CSNPs loaded 3 μg/mL coumarin-6 for 1 h and 1 μg/mL coumarin-6 for 3 h showed stronger fluorescence, which indicated that more coumarin-6 was uptaken, that is to say, the uptake of CSNPs was time-dependent and concentration-dependent. This result was consentient with the uptake behavior studies performed up to date.[40] Moreover, it indicated that concentration contributed more to the uptake of CSNPs by PC3 cells than time, which was just opposite to A549 cells, suggesting that different types of cells owned different uptake behavior.

The fluorescence was examined by FACS and the data was also presented in Figure 6. Flow cytometry profile presented the relative intensity of fluorescence signal in X axis and the relative number of cells in Y axis. The results were respectively consistent with those of the CLSM images.

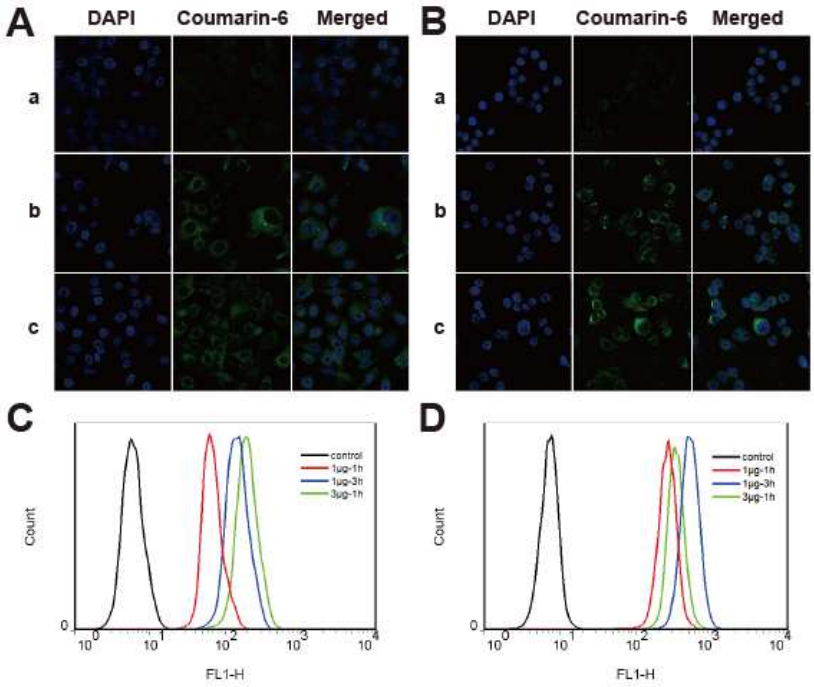

Figure 6. Cellar uptake of coumarin-6-loaded CSNPs in PC3 and A549 cells (n = 3). The CLSM images of PC3 cells (A) and A549 cells (B) treated with coumarin-6-loaded CSNPs at different times and concentrations: 1 h (1 μg/mL, a), 3 h (1 μg/mL, b), 1 h (3 μg/mL, c). Cells were counterstained with DAPI (for nuclei). Flow cytometry profile of PC3 cells (C) and A549 cells (D) presented the relative intensity of fluorescence signal in X axis and the relative number of cells in Y axis. Black line: control, red line: CSNPs containing 1μg/mL coumarin-6 for 1 h, blue line: CSNPs containing 1 μg/mL coumarin-6 for 3 h, green line: CSNPs containing 3 μg/mL coumarin-6 for 1 h.

Cell Cycle Analysis. Cabazitaxel has been reported to target tubulin and inhibit depolymerization of microtubules, which results in cell-cycle arrest.[4] Hence, cell-cycle arrest effects of cabazitaxel solutions, CSNPs and citronellol solutions were investigated. Cell cycle tests were performed using a KeyGEN Cell Cycle Detection Kit and tested by FACS, and the results were presented in Figure 7. Compared with control group, it was obvious that more PC3 and A549 cells treated with cabazitaxel solutions and CSNPs were accumulated in G2/M phases and fewer in G0/G1 phases by a concentration dependent manner. In particular, compared with cabazitaxel solutions, CSNPs induced slightly fewer cells arrest in the G2/M phase and both cabazitaxel solutions and CSNPs had more cell-arrest effects in PC3 cells than A549 cells. And citronellol solutions induced very little cells arrest in the G2/M phase in both PC3 and A549 cells. All these results are concordant with the data acquired by MTT analysis and suggesting that the CSNPs can effectively block the mitosis at G2/M phase.

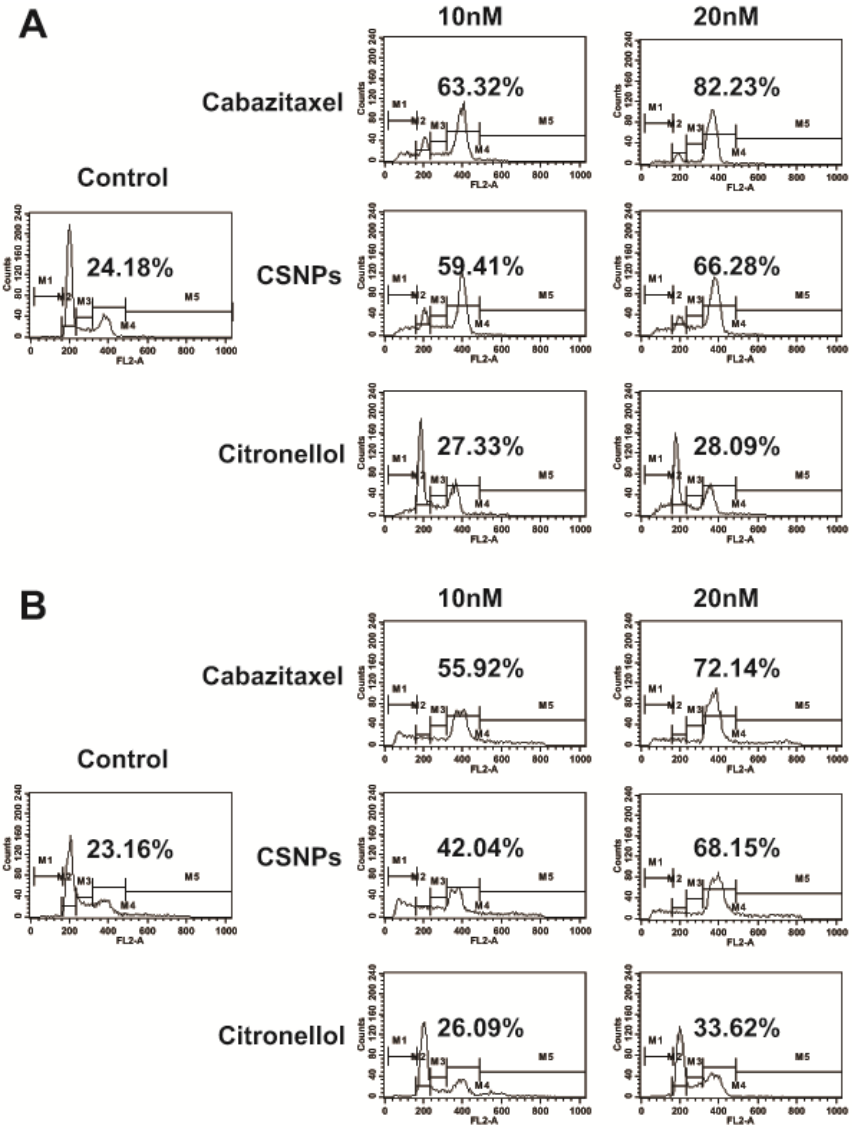

Figure 7. Effects on the cell cycle of PC3 cells (A) and A549 cells (B) treated with cabazitaxel solutions, CSNPs and citronellol solutions (n = 3). The test groups were incubated with equivalent cabazitaxel of 10 nM and 20 nM for 24 h. And the control groups were incubated with only fresh media for 24 h.

Cell Apoptosis Study. Cell apoptosis test was performed using a BD Annexin V-Fluorescein Isothiocyanate Apotpsis Detection Kit and tested by FACS, and the results were presented in Figure 8. To measure the quantitative apoptosis effects of cabazitaxel solutions, CSNPs and citronellol solutions, AnnexinV-FITC/PI was used to co-stain the cells, which could distinguish living cells from dead cells or early

apoptosis cells from late apoptosis ones. In the flow cytometry profiles, the lower left, upper left, lower right and upper right quadrants denoted live, necrotic, early apoptotic and late apoptotic regions, respectively.

In Figure 8A, most PC3 cells treated with formulations were live and a large part was on the stage of early apoptosis with increased concentration. Markedly, citronellol solutions induced many cells apoptosis, although fewer than that induced by cabazitaxel solutions and CSNPs, which might be the reason why cabazitaxel solutions and CSNPs caused almost the same number of apoptosis including early and late apoptosis. In Figure 8B, it showed that cabazitaxel solutions and CSNPs were more effective to A549 cells than to PC3 cells, which may be because A549 cells can take in more drugs than PC cells. And most A549 cells treated with cabazitaxel solutions and CSNPs were on early apoptosis, which was also concentration-dependent. However, citronellol solutions induced scarcely cell apoptosis.

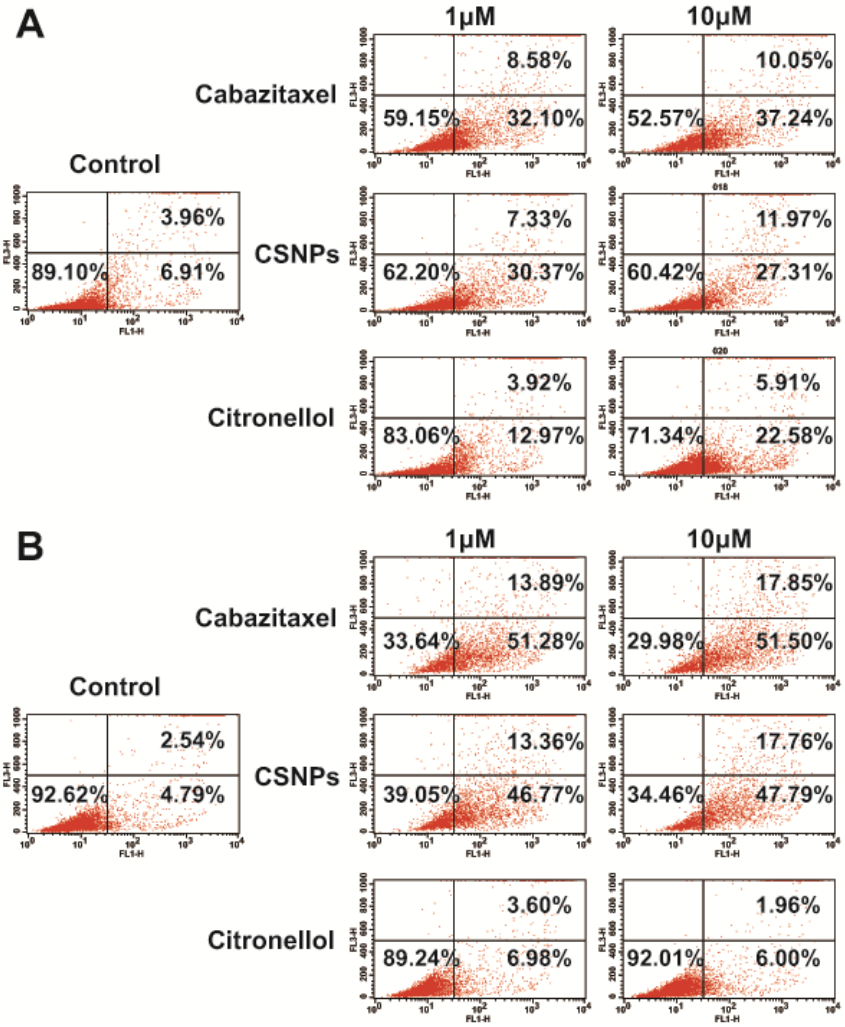

Figure 8. Induction of apoptosis on PC3 cells (A) and A549 cells (B) by cabazitaxel solutions, CSNPs and citronellol solutions (n = 3). Apoptosis was evaluated after cells treated with cabazitaxel solutions, CSNPs or citronellol solutions containing 1 μM and 10 μM drugs for 48 h. Flow cytometry profile showed PI in Y axis and Annexin-V-FITC in X axis. The normal cells were showed in the lower left quadrant, the late apoptotic cells were showed in the upper right quadrant and the early apoptotic cells were showed in the lower right quadrant.

***In Vivo* Pharmacokinetics and Biodistribution.** The main pharmacokinetic parameters of cabazitaxel in rats after intravenous administration of cabazitaxel solutions and CSNPs were summarized in Table S3. And the plasma concentration–time curves of cabazitaxel were shown in Figure 9A. The results indicated that there was an apparent difference for main pharmacokinetic parameters, AUC_{0-t} and $t_{1/2}$,

between cabazitaxel solutions and CSNPs. The AUC_{0-t} for CSNPs was 2717.6 ± 989.1 ng·h/mL which was 6.5-fold higher than that of cabazitaxel solution (420.3 ± 83.9 ng·h/mL), demonstrating that the self-assembled nanoparticles was stable and pegylation can reduce the clearance of CSNPs from the body. Compared with cabazitaxel solutions, the half-time of CSNPs was also increased to 6.7 ± 1.8 h (2.3-fold increase) implying that the blood circulation time of cabazitaxel was prolonged.

To explore whether CSNPs can effectively improve the accumulation in tumor, the in vivo targeting property of the CSNPs was investigated in tumor-bearing A549 nude mice. The common used near infrared fluorescence dye DiR loaded by CSNPs was selected to reflect the distribution of CSNPs in the body after intravenous administration. The DiR solutions and DiR-loaded CSNPs were injected into mice with a dose of 2 mg/kg, respectively. At desired time points, three mice were imaged in vivo in each group, and other two mice were sacrificed and the major organs and tumor were harvested for ex vivo imaging at 4 h, 24 h post-injection in each group. And the results of the fluorescence imaging at predetermined time intervals of only one live mouse for each group were exhibited in Figure 9B. Apparently, the fluorescence of mice treated with DiR solutions was mainly detected at liver and had increased in lung with time pasted. For DiR-loaded CSNPs, although there was still high level of fluorescence in the liver, strong fluorescence can be found at the tumor site at desired time intervals. The same result was observed in Figure 9C, for control group, the fluorescence was major in the liver at 4 h post-treatment and not detected in tumor. Even 24 h post-administration, there was still no fluorescence can be found in tumor and there were high levels of fluorescence in the liver and lung. The results indicated most of DiR were captured by RES and accumulated at liver and lung sites. Other researches were also reported the RES is the major obstacle for many

antitumor-drugs due to its non-specific defense mechanisms.[41-43] As for the DiR-loaded CSNPs group, the fluorescence in the tumor can be apparently observed. Although liver has strong fluorescence, low levels of fluorescence were detected in heart, spleen, lung and kidney. These results demonstrated that CSNPs have effect on reducing the RES uptake and improving tumor biodistribution.

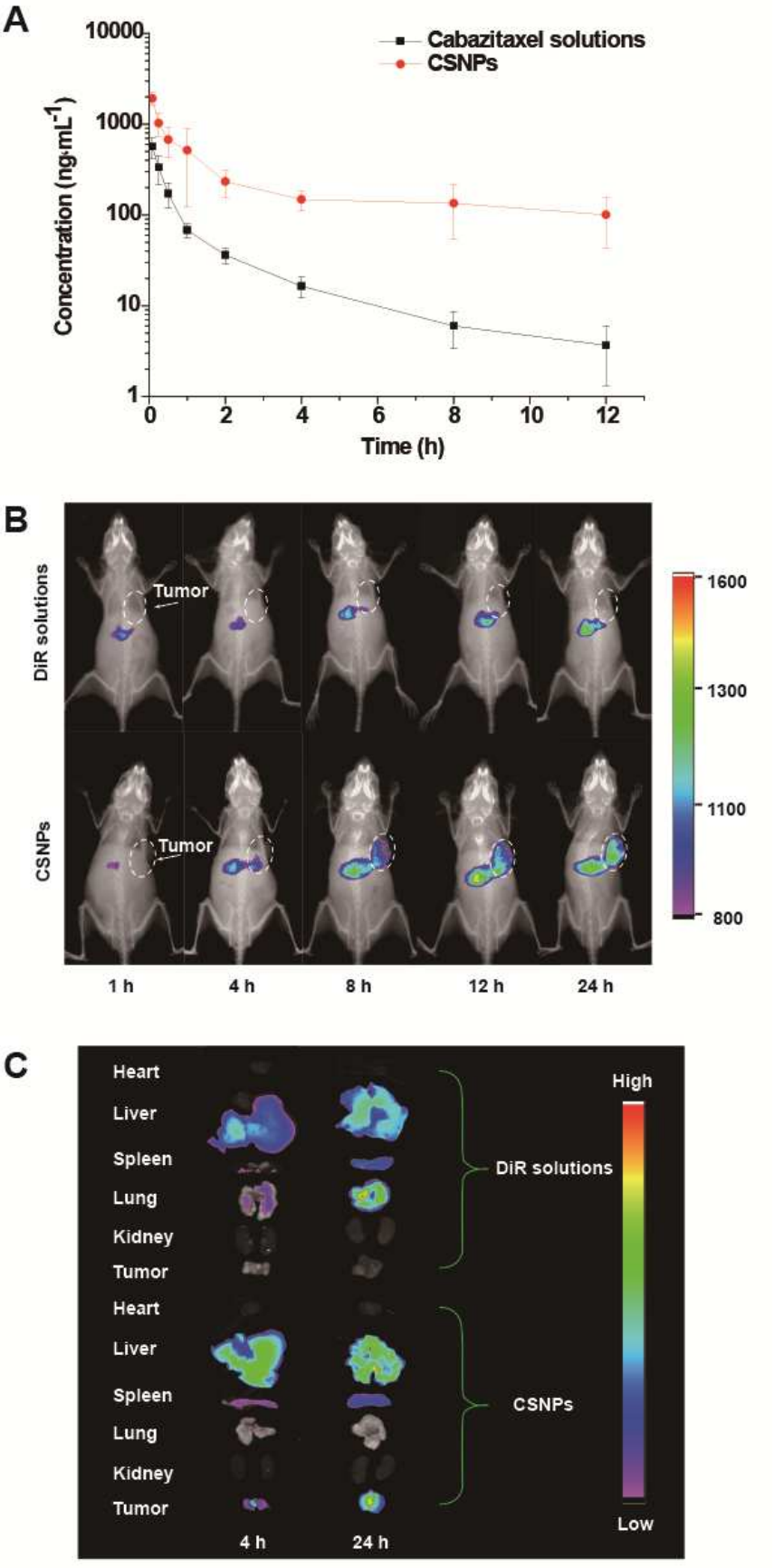
A
Cabazitaxel solutions
CSNPs
Concentration (ng·mL-1)
10000
1000
100
10
1
0
2
4
6
8
10
12
Time (h)
B
DiR solutions
CSNPs
Tumor
Tumor
1600
1300
1100
800
1 h
4 h
8 h
12 h
24 h
C
Heart
Liver
Spleen
Lung
Kidney
Tumor
DiR solutions
High
Heart
Liver
Spleen
Lung
Kidney
Tumor
CSNPs
Low
4 h
24 h

363

Figure 9. Plasma concentration-time profiles of cabazitaxel after intravenous administration of cabazitaxel solutions and CSNPs of the equivalent cabazitaxel dose (3 mg/kg) in rats (mean ± SD, n = 5) (A). In vivo fluorescence imaging of tumor-bearing A549 nude mice at predetermined time intervals post-injection of DIR-solutions and DIR-loaded CSNPs (B). Ex vivo fluorescence imaging of tumor and major organs taken from tumor-bearing A549 nude mice at 4 h and 24 h time points (C).

Preparation and Characterization of Curcumin-loaded CSNPs. The CSNPs can be used as a redox-responsive nanocarrier for other anticancer drugs for rapidly release, providing an attractive approach for releasing drug within tumor cells and combination therapy. In this study, curcumin, a hydrophobic drug that has diverse effects including cytotoxicity[26,27] was loaded by CSNPs. The mixed ethanol solutions of curcumin and citronellol-cabazitaxel conjugate were added into water and stirred for 1 min to form the curcumin-loaded CSNPs. The particle size, size distribution and Zeta potential analysis of curcumin-loaded CSNPs were carried out by DLS, showing that the CSNPs had small particle size of 129.7 ± 3.04 nm, a fair PDI of 0.076 ± 0.064 and mean Zeta potential of -24.5 ± 0.17 (Table S1), and TEM revealed that curcumin-loaded CSNPs were spherical and similar with CSNPs (Figure S1B). The curcumin-loaded CSNPs with drug loading content of 7.98 ± 0.07 wt% (curcumin) and 56.33 ± 0.04 wt% (cabazitaxel) and entrapment efficiency of 83.22 ± 0.77%, implied that the CSNPs can successfully encapsulate curcumin and have high entrapment efficiency, which was not reported before. Compared with other strategies for codeliver drugs, such as using PLGA nanoparticles co-loaded with paclitaxel and Stat3 siRNA,[44] lipid-albumin nanoassemblies codeliver paclitaxel and borneol,[45] core-matched nanoemulsions codeliver paclitaxel and 5-fluoroucacil,[46] the multifunctional CSNPs showed apparent advantage that can increase the capability of loading drugs. Moreover, the long term stability study of curcumin-loaded CSNPs (Figure S1C) was

investigated at 4 °C. The results determined by DLS suggested there were no obvious changes in particle size and PDI of the nanoparticles after several weeks. Therefore, the structure of curcumin-loaded CSNPs was stable.

***In Vitro* Anti-tumor Effect of Combined Therapy.** Figure 10 showed that curcumin had no cell inhibition-effect on both PC3 and A549 cells at concentration varying from 0.001 nM to 10 nM. However, the employment of curcumin in curcumin-loaded CSNPs could effectively enhance the anti-tumor effect of citronellol-cabazitaxel conjugate. Curcumin-loaded CSNPs showed slight synergistic anti-tumor effects on both PC3 and A549 cells at concentration varing from 0.001 nM to 1 nM. Notablely, at concentration from 1 nM to 10 nM curcumin-loaded CSNPs presented strong synergistic effects for inhibiting PC3 and A549 cells, and the cell inhibition reached 91.8% and 90.5% at 10 nM on PC3 and A549 cells, respectively compared with CSNPs (53.8% and 44.7%, respectively). The IC_{50} of curcumin-loaded CSNPs on PC3 and A549 cells were 0.02 ± 0.01 nM and 0.28 ± 0.03 nM, respectively compared with CSNPs (0.70 ± 0.04 nM and 4.33 ± 0.27 nM, respectively) (Table S4). In fact, the quantity of both curcumin (≤ 3.9 nM) and citronellol-cabazitaxel conjugate (≤ 10 nM) was very small. Hence, the synergistic anti-tumor effects of curcumin and citronellol-cabazitaxel conjugate in curcumin-loaded CSNPs could be significantly employed in enhancing the anti-tumor effect, reducing the amount of drugs, thereby reducing the incidence of side effects.

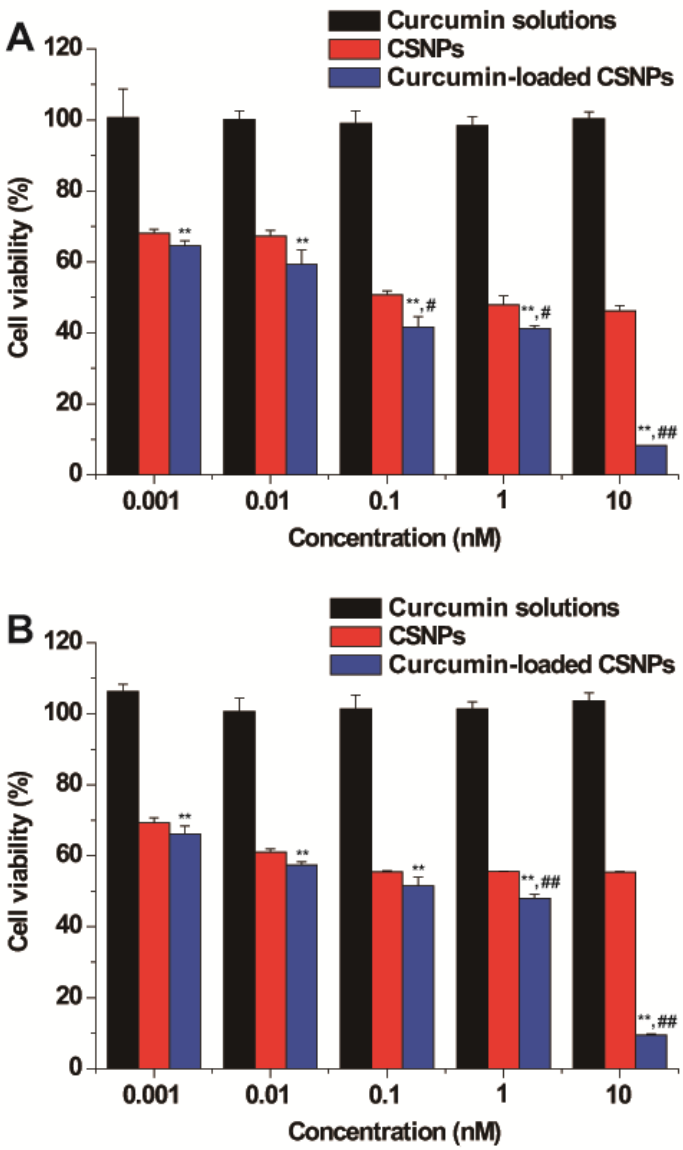

Figure 10. The koinonia by MTT assays of curcumin, CSNPs and curcumin-loaded CSNPs on PC3 cells (A) and A549 cells (B). The cells were incubated with preparations for 48 h at concentrations varying from 0.001 nM to 10 nM. Data are presented as mean ± SD (n = 3). **: compared with curcumin solutions, $P < 0.01$; #: compared with CSNPs, $P < 0.05$; ##: compared with CSNPs, $P < 0.01$.

CONCLUSIONS

In conclusion, we have successfully synthesized a novel disulfide-linked cabazitaxel prodrug by conjugating cabazitaxel with citronellol via the disulfide bond, and the citronellol-cabazitaxel conjugate self-assembled nanoparticles were prepared. Notably, the CSNPs have several unique features: (a) The preparation method is simple and the CSNPs are stable spherical nanoparticles with uniform size distribution. (b) The loading content of cabazitaxel in CSNPs is significantly higher than other biocompatible nanosystems such as polymeric micelles and polymeric nanoparticles. (c) The disulfide bond is redox-responsive so that the CSNPs can reduce the general toxicity and rapidly release cabazitaxel within tumor cells. (d) The cell uptake of CSNPs is both time-dependent and concentration-dependent. And CSNPs can block the mitosis at G2/M phase and induce the apoptosis of PC3 and A549 cells that produce higher antitumor effect. (e) The *in vivo* pharmacokinetics of CSNPs is apparently improved, and the CSNPs have target effect for accumulating at tumor site.

Furthermore, CSNPs exhibit an excellent property that can load other hydrophobic drugs or imaging agents. In this article, fluorescence dyes 6-coumarin and DiR were successfully loaded in CSNPs for the experiment of cell uptake and *in vivo* biodistribution of CSNPs, respectively. And curcumin-loaded CSNPs were also prepared and expressed strong synergistic anticancer effects. All these results indicate that the redox-sensitive citronellol-cabazitaxel conjugate can be utilized as a smart multifunctional nanomedicine for combination cancer therapy and theranostics.

EXPERIMENTAL PROCEDURES

Materials. Cabazitaxel (CTX) was purchased from Beijing Maisuo Chemical Technology Co Ltd (Beijing, China). Citronellol (CIT) was obtained from Chengdu Gracia Chemical Technology Co. Ltd. (Chengdu, China). Dithiodiglycolic acid (DTDA), 4-Dimethylaminopyridine (DMAP) and phenylmethanesulfonyl fluoride (PMSF) were bought from Aladdin Industrial Corporation (Shanghai, China). 1-Ethyl-3-(3-dimethyllaminopropyl)carbodiimide hydrochloride (EDCI) and 1-Hydroxybenzotriazole (HOBt) were purchased from Energy Chemical Co. Ltd. (Shanghai, China). 2-distearoyl-snglycero-3-phosphoethanolamine-N-[methoxy(polyethylene glycol)-2000] (DSPE-PEG2000) was obtained from Shanghai Advanced Vehicle. The human lung cancer cells (A549) and human prostatic carcinoma cells (PC3) were purchased from the cell bank of Chinese Academy of Sciences (Beiijng, China). Roswell Park Memorial Institute (RPMI-1640), Dulbecco's Modified Eagle Medium (DMEM, high glucose), trypsin and 3-(4,5-dimethylthiazol-2-yl)-2,5-diphenyltetrazoliumbromide (MTT) were obtained from Gibco (Beijing, China). Nutrient Mixtuee F-12 Ham Kaghn's Modification (F12K) and Coumarin-6 were purchased from Sigma (St. Louis, MO, USA). Fetal bovine serum (FBS) and CS were purchased from Hyclone (Beijing, China) and KeyGEN (Nanjing, China), respectively. Dimethylsulfoxide (DMSO) was purchased from Kemeng (Tianjin, China). 1,1-dioctadecyl-3,3,3,3-tetramethylindotricarbocyanine iodide (DiR) and 4′,6-diamidino-2-phenylindole (DAPI) were brought from AAT Bioquest (Beiijng, China) and Beijing Founction biotechnology company (Beiijng, China), respectively. Isoflurane was bought from RWD life science Co. Ltd. (Shenzhen, China). Curcumin was purchased from Sinopharm Chemical Reagent Co. Ltd. (Beijing, China)All other reagents and solvents used in this article were of analytical grade.

Synthesis of Citronellol-cabazitaxel Conjugate. DTDA (0.5 g, 2.74 mmol) and 2 mL acetic anhydride were added to a 100 mL round-bottom flask equipped with a magnetic stirrer. The mixture was stirred for 2 hours at 25 ℃ under nitrogen atmosphere. Thereafter, 20 mL methylbenzene was repeatedly added and then dried in vacuo (< 30 ℃) for three times. The crude product was subjected to the subsequent step without further purification. The anhydride was dissolved in 20 mL anhydrous dichloromethane, and then citronellol (0.17 mL, 0.928 mmol) and DMAP (13 mg, 0.106 mmol) were added. The reaction was stirred at 25 ℃ for 1 h and the completion of reaction was monitored by TLC (Hex/EA = 1:1). The crude product was collected by filtration and dried in vacuo (< 30 ℃) as a yellow oily solid (0.627 g). It was purified by silica gel column chromatography (Hex/EA = 5:1，1 ‰ HOAc) to give a light yellow solid compound (CIT-DTDA, 0.26 g, 87.9%). CIT-DTDA(56 mg, 0.175 mmol)，EDCI (40 mg, 0.209 mmol)，HOBt (28 mg, 0.209 mmol and DMAP (6 mg, 0.049 mmol) in 4 mL anhydrous dichloromethane were stirred at -5~-8 ℃ for 1 h under nitrogen atmosphere, then cabazitaxel (150 mg, 0.179 mmol) was added to the reaction liquid, and the mixture was further stirred at 25 ℃ for 4 h under nitrogen atmosphere. The completion of reaction was tested by TLC (Hex/EA = 1:1). The reaction liquid was extracted by water (20 mL × 3) and the organic phase was dried by anhydrous sodium sulfate. The crude product was purified by HPLC to obtain citronellol-cabazitaxel conjugate (169 mg, 82.8%) as a white solid.

^{1}H NMR spectra was recorded on a Bruker ARX-400 NMR spectrometer operating at 400 MHz and using deuterated chloroform ($CDCl_3$) as a solvent. The chemical shifts were corrected against residual solvent signals. The accurate mass of sample was performed using a Bruker micrOTOF-Q time of flight mass spectrometer, mass range of m/z was 50 ~ 3000, ion type is $[M + Na]^+$.

Preparation and Characterization of CSNPs. CSNPs were prepared via the existing nano-precipitation method.[22] Briefly, The ethanol solution containing 10 mg/mL citronellol-cabazitaxel conjugate was slowly added into water that was stirred (800 rpm) at room temperature. After 1 min, the self-assembled nanoparticles (containing 2 mg/mL citronellol-cabazitaxel conjugate) were formed and 10 mg/mL DSPE - PEG2000 (20%, w/w) was then slowly added to the solution for pegylation. The CSNPs were stored at 4 ℃.

The size and Zeta potential of the CSNPs were measured by DLS. The measurements that performed in triplicate were carried out via a Zetasizer (Nano ZS, Malvern. UK and the results were evaluated by mean ± standard deviation (SD). The morphology of CSNPs was observed through TEM (JEM2100, JEOL. Japan) operated at an accelerating voltage of 200 kV. The samples were prepared by dropping 10 μL of nanoparticle solution on a carbon-coated copper grid for 3 min and then dried by filter paper. Finally, 1% uranyl acetate (5 μL) was dropped for 30 seconds and air dried.

The Mechanism of the Conjugate to Self-assemble into Nanoparticles. A simple study to explore the mechanism of the conjugate to self-assemble into nanoparticles was conducted by imaging the dynamics of crystal growth. Ethanol containing cabazitaxel and citronellol-cabazitaxel conjugate was placed onto a glass slide, respectively. After drying and desiccating, add a drop of water to each sample. Pictures were taken after the slides were kept in a humidified chamber at room temperature for 6 h.

To investigate self-assembly interaction among molecules, computational simulation was also used. The citronellol-cabazitaxel conjugate structures were constructed by package and optimized with the material studio 8.0 software. All

molecular dynamics (MD) simulations were performed by using the Amorphous Cell and Forcitemodule of the Material studio simulation package with COMPASS. In the MD simulation, firstly, amorphous cell module was employed to construct a box, which was inundated with 200 water molecules and 4 citronellol-cabazitaxel conjugate molecules. Then, 100 ns MD simulations were performed under the constant temperature of 200 K. The results were displayed in accompanying Supporting Information.

***In Vitro* Drug Release Study.** The release of cabazitaxel from CSNPs and the degradation of citronellol-cabazitaxel conjugate were studied under shaking (100 rpm) at 37 °C in four different media which were the phosphate buffer saline (PBS, pH 7.4) containing 0.5% Tween 80 with 10 mM, 1 mM, 10 μM and 1 μM GSH, respectively. Typically, 1 mL of CSNPs dispersions (2 mg/mL) was added to 25 mL of release media. The release studies were conducted at different time intervals: 1, 2, 3, 6, 12 and 24 h. At desired time intervals, 1 mL samples was withdrawn and replenished with the equal volume of fresh media. The content of cabazitaxel and citronellol-cabazitaxel conjugate was determined by high-performance liquid chromatography (HPLC) with Waters e2695 Separations Module and Waters 2489 UV/Visible Detector on a reverse ODS Cosmosil-C18 column (250 mm × 4.6 mm, 5 μm) thermostated at T = 40 °C with UV detection at 227 nm using a mixture of acetonitrile/water (80:20, v/v) as a mobile phase with a flow rate of 1 mL/min. Each experiment was repeated in triplicate and the results were expressed by mean ± SD.

Rat Plasma Stability. The stability of CSNPs in rat plasma was analyzed by incubating CSNPs in rat plasma without or with polymethylsulfonyl flouride (PMSF, 2.5 mM). In each group, CSNPs were mixed with rat plasma to reach the concentration of 50 μg/mL and stored at 37 °C. At desired time intervals, 100μL

samples was taken out and processed according to the operation steps of pharmacokinetic study for measuring the content of citronellol-cabazitaxel conjugate. Each experiment was repeated in triplicate and the results were displayed in accompanying Supporting Information.

Cell Culture. A549 lung cancer cells and PC3 human prostatic carcinoma cells were cultured in RPMI Medium 1640 and F12K, respectively with 10% fetal bovine serum (FBS), 100 μg/mL streptomycin and 100 units/mL penicillin in a humidified cell culture incubator at 37 °C, 5% CO_2. The cells were subcultured by 0.25% trypsin without EDTA when grown up to 80%.

Cell Viability Assay. The antitumor activity of formulations was evaluated by MTT assays. PC3 and A549 cells were seeded in a 96-well plate (5000 cells/100 μL/well and 3000 cells/100 μL/well, respectively) and cultured at 37 °C, 5% CO_2. Next day, the media was removed and then replaced with fresh media containing series of concentrations of formulations. Cabazitaxel and citronellol were dissolved by DMSO and then diluted by fresh media, respectively. The final concentration of DMSO was 0.1%, meanwhile, the control group also contained 0.1% DMSO. CSNPs were diluted by fresh media directly, with fresh media as the control group. When the cells were cultured for 48 h, the media was displaced by another 100 μL fresh media, then, 15 μL of MTT reagent (5 mg/mL) was added to the media and the cells were incubated continuously for 4h. Then the media was replaced with 100 μL DMSO and vibrated for 10 min. The absorbance at 570 nm of each well was measured on a microplate reader. Eq. (1) was employed to calculate the cell inhibition rate:

$$\text{Cell inhibition rate (\%)} = 1 - A_e/A_c \quad (1)$$

In Eq. (2), A_e is the mean absorbance of the experimental group and A_c is the mean absorbance of the control group. The IC_{50} values were calculated by SPSS software.

Cell Uptake Study. 6-coumarin-loaded CSNPs were prepared via the similar way with previously described but changed the ethanol solution of citronellol-cabazitaxel conjugate to the mixture of 6-coumarin and citronellol-cabazitaxel conjugate (6-coumarin: citronellol-cabazitaxel conjugate = 1:10, w/w) to study the effect of concentration and time on the uptake of CSNPs by cells. Cells were seeded on a 6-well plate at a density of 3×10^5 cells/2 mL/well and allowed to adhere overnight. Afterwards, CSNPs containing 1 μg/mL (for 1 h and 3 h, respectively) and 3 μg/mL (for 1 h) 6-coumarin were added to wells. Then cells were collected and analyzed by FACS.

The cellular uptake was also studied by confocal laser scanning microscope (CLSM, C2SI, Nikon, Japan). Cells were seeded on a 24-well plate every well of which contained a coverslip at a density of 3×10^4 cells/1 mL/well and allowed to adhere for 24 h. Then the cells were treated with CSNPs containing 1 μg/mL (for 1 h and 3 h, respectively) and 3 μg/mL (for 1 h) 6-coumarin diluted by the fresh culture medium. After that, the cells were washed twice with PBS, fixed with 4% paraformaldehyde for 10 min at room temperature and washed twice with PBS again. Following, cells were treated with 0.5% paraformaldehyde for 10 min and washed with PBS twice. The nuclei were dyed with DAPI for 1 h at 37 °C and washed with PBS twice. Finally, the coverslips were fixed on slide glass and observed by the CLSM.

Cell Cycle Analysis. The effect of formulations on cell cycle was determined by KeyGEN Cell Cycle Detection Kit. Cells were seeded in a 6-well plate at a density of 3×10^5 cells/2mL/well and allowed to attach for 1d. Then the media was replaced with cabazitaxel solutions, citronellol solutions or CSNPs of different concentrations diluted with fresh media. After 24 h, cells were gathered, washed and fixed overnight in the 70% ethanol PBS solution at -20 ℃. Next day, cells were washed and handled

by 100 μL RnaseA at 37 °C for 30 min and then stained with propidium iodide (PI) solution at 4 °C for 30 min. 10000 events were tested on a flow cytometer (FACS) every sample.

Cell Apoptosis Study. The apoptosis analysis of different formulations was performed by BD Annexin V-Fluorescein Isothiocyanate Apotpsis Detection Kit 1. Cells were seeded in a 6-well plate (3×10^5 cells/2mL/well). Next day, the media was taken away and cells were cultured in fresh media comprising cabazitaxel solutions, citronellol solutions or CSNPs, respectively for 48 h. After that, cells were collected and stained by Annexin V-Fluorescein Isothiocyanate and PI and analyzed by FACS.

Pharmacokinetic Study. The Sprague–Dawley rats weighing 200-220 g (Laboratory Animal Center of Shenyang Pharmaceutical University, Shenyang, Liaoning, China) were employed in the pharmacokinetics studies. The rats were divided into two groups and were injected via lateral saphenous vein with cabazitaxel solutions and CSNPs of the equivalent cabazitaxel dose (3 mg/kg, n = 5), respectively. About 400 μL of blood samples were collected at different time points (0.083 h, 0.25 h, 0.5 h, 1 h, 2 h, 4 h, 6 h, 8 h, 12 h and 24 h) post-injection, and were centrifuged to obtain the serum, the concentration of cabazitaxel in blood was measured by ultraperformance liquid chromatography/tandem mass spectrometry (UPLC-MS/MS). 50 μL plasma samples was transferred to a 10.0 mL vial, added with 10 μL docetaxel working solution (internal standard) and vortex mixed for 1min. Analytes were extracted by using 1.0 mL TBME, then vortex mixed for 3min and centrifuged for 5 min at 3500 rpm. The organic upper layer was removed and evaporated to dryness under slow flow of N_2 at 37 °C. Dried extracts were redissolved in 100 μL methanol : water (4:1, v/v) and vortex mixed for 2 min. Samples were centrifuged for 5 min at 13,000 rpm. The supernatant was transferred into an autosampler vial with insert.

The parameters of tandem mass spectrometry were set as follows: The ion spray voltage was kept at 4.10 kV and the cone voltage at 40 V in the positive ion electro spray ionization mode. m/z 857.9 > 577.2, collision energy at 20 V for cabazitaxel and m/z 830.1 > 548.9, collision energy at 25 V for internal standard. Analytes were separated on a Phenomenex C18 column (50mm × 2.1mm, 2.6μm) thermostatted at T = 35 °C. The mobile phase consisted of a mixture of methanol (mobile phase A) and 0.2% phosphoric acid (mobile phase B) was used at a flow rate of 0.2 mL/min. A linear gradient was applied, with 50-85% mobile phase A, from 0 to 1.3 min, followed by keeping the eluent composition for 0.5 min. Then the mobile phase A back to 50% from 1.8 to 2.3 min, which was held for 0.5 min to re-equilibrate.

***In Vivo* Targeting Effect.** The tumor biodistribution of CSNPs was assessed by tumor-bearing A549 mice (Laboratory Animal Center of Shenyang Pharmaceutical University, Shenyang, Liaoning, China) using the FX Pro *in vivo* imaging system (Carestream Health). The near infrared fluorescence dye DiR was loaded in CSNPs for near-infrared (NIR) fluorescence imaging. Tumor-bearing mice were established by injecting a suspension of 1×10^6 A549 cells in PBS into the right flank of BALB/C mice. Mice with subcutaneous tumors of approximate 100-150 mm^3 were subjected to treatment. DiR-loaded CSNPs was injected intravenously via the tail vein into the tumor-bearing mice to trace profiles of the tumor accumulation and biodistribution of CSNPs. Three mice were *in vivo* imaged at predetermined time intervals in each group. And other two mice were sacrificed at 4 h and 24 h respectively in each group and the *ex vivo* biodistribution imaging signals of DiR in each organ and tumor were immediately detected.

Preparation and Characterization of Curcumin-loaded CSNPs. Curcumin-loaded CSNPs (curcumin : citronellol-cabazitaxel conjugate = 1:8, w/w) were

prepared as previously described. The entrapment efficiency (EE) was analyzed by centrifugal ultrafiltration method, which 200 μL curcumin-loaded CSNPs were added in ultrafiltration centrifugal tube (100 kDa) and then centrifuged (3500 rpm) for 30 min that leaded to the free drug flows to the bottom, and the content of curcumin was determined through HPLC on a reverse ODS Cosmosil-C18 column (250 mm × 4.6 mm, 5 μm) thermostated at T = 35 °C with UV detection at 420 nm using a mixture of acetonitrile/water/phosphoric acid (60:40:0.2, v/v) as mobile phase at a flow rate of flow 1 mL/min. EE and drug loading content (DLC) were calculated according to the following formula:

$$EE\ (\%) = (1-C_f/C_t)\times 100\% \quad (2)$$

$$DLC\ (wt\%) = W_d/W_t\times 100\% \quad (3)$$

In Eq. (2), C_f and C_t are the content of the free drug and the total drug of CSNPs, respectively. And in Eq. (3), W_d is the weight of drug loaded in CSNPS and W_t is the weight of drug-loaded CSNPS.

The Size and Zeta Potential of the curcumin-loaded CSNPs were determined by DLS as previously described. The sample was also imaged by TEM. Long-term stability study of the CSNPs loading curcumin or not was carried out at 4 °C without special shaking. The solution was analyzed by DLS at different day among 60 days. Particle size and polydispersity index (PDI) were used to evaluate the stability of the CSNPs.

***In Vitro* Anti-tumor Effect of Combination Therapy.** The synergistic antitumor effects on both PC3 and A549 cells were investigated by MTT assays of curcumin, CSNPs and curcumin-loaded CSNPs at concentration varing from 0.001 nM to 10 nM. The processing method was the same as the previous MTT experiment.

Statistical Analysis. All the results were represented as mean ± SD. The statistical significance was determined using SPSS software. $P < 0.05$ was considered significant, and $P < 0.01$ was considered highly significant.

AUTHOR INFORMATION

Corresponding Author

*Fax: +86-24-23986325. E-mail: wangyjspu@163.com.

Notes

The authors declare no competing financial interest.

ACKONWLEDGMENTS

This work was supported by the National Nature Science Foundation of China (No. 81273450), Nature Science Foundation of Liaoning Province (No. 2014020079), and the General Project in Education Department of Liaoning Province (No. L2014396).

ASSOCIATED CONTENT

Supporting Information

Characteristics of CSNPs and curcumin-loaded CSNPs (Table S1). The morphology and store stability of curcumin-loaded CSNPs (Figure S1). Characterization of the formation and structure of self-assembled particles (Figure S2). Stability of cabazitaxel in PBS (pH 7.4) at 37 ℃ under four different conditions of GSH (Figure S3). Stability of CSNPs in rat plasma with PMSF (2.5 mM) and without PMSF at 37 ℃ (Figure S4). IC_{50} of PC3 and A549 cells incubated with cabazitaxel solutions and CSNPs at 48 h (Table S2). The comparison between additional effect and combinational effect of citronellol and cabazitaxel on PC3 and A549 cells by MTT assays. (Figure S5). Observation of the solutions of coumarin-6, coumarin-6 loaded CSNPs and CSNPs (Figure S6). Pharmacokinetic parameters of cabazitaxel after intravenous administration of cabazitaxel solutions and CSNPs (Table S3). IC_{50} of

PC3 and A549 cells incubated with CSNPs and curcumin-loaded CSNPs at 48 h (Table S4). This material is free of charge on Internet at http://pubs.acs.org.

REFERENCES

(1) Scher, H. I. (2008) Design and End Points of Clinical Trials for Patients With Progressive Prostate Cancer and Castrate Levels of Testosterone: Recommendations of the Prostate Cancer Clinical Trials Working Group. *J. Clin. Oncol.* 26, 1148-1159.

(2) Yoneda, T. (1998) Cellular and molecular mechanisms of breast and prostate cancer metastasis to bone. *Eur. J. Cancer* 34, 240-245.

(3) Pivot, X., Koralewski, P., Hidalgo, J. L., Chan, A., Gon04alves, A., Schwartsmann, G., Assadourian, S., and Lotz, J. P. (2008) A multicenter phase II study of XRP6258 administered as a 1-h i.v. infusion every 3 weeks in taxane-resistant metastatic breast cancer patients. *Ann. Oncol.* 19, 1547-1552.

(4) Galsky, M. D., Argyris, T., Peter, K., and Oh, W. K. (2010) Cabazitaxel. *Nat. Rev. Drug Discov.* 9, 677-678.

(5) Bono, J. S. d., Oudard, S., Ozguroglu, M., Hansen, S., Machiels, J.-P., Kocak, I., Gravis, G., Bodrogi, I., Mackenzie, M. J., and Shen, L. (2010) Prednisone plus cabazitaxel or mitoxantrone for metastatic castration -resistant prostate cancer progressing after docetaxel treatment: a randomised open -label trial. *Lancet* 376, 1147–1154.

(6) Kartner, N., Riordan, J. R., and Ling, V. (1983) Cell surface P-glycoprotein associated with multidrug resistance in mammalian cell lines. *Science* 221, 1285-1288.

(7) Abidi, A. (2013) Cabazitaxel: A novel taxane for metastatic castration-resistant prostate cancer-current implications and future prospects. *J. Pharm. Pharmacother.* 4, 230-237.

(8) Gou, J., Feng, S., Xu, H., Fang, G., Chao, Y., Zhang, Y., Xu, H., and Tang, X. (2015) Decreased core crystallinity facilitated drug loading in polymeric micelles without affecting their biological performances. *Biomacromolecules* 16, 2920-2929.

(9) Song, Y., Tian, Q., Huang, Z., Fan, D., She, Z., Liu, X., Cheng, X., Yu, B., and Deng, Y. (2014) Self-assembled micelles of novel amphiphilic copolymer cholesterol-coupled F68 containing cabazitaxel as a drug delivery system. *Int. J. Nanomedicine* 9, 2307-2317.

(10) Xie, C., Zhang, P., Zhang, Z., Yang, C., Zhang, J., Wu, W., and Jiang, X. (2015) Drug-loaded pseudo-block copolymer micelles with a multi-armed star polymer as the micellar exterior. *Nanoscale* 7, 12572-12580.

(11) Diou, O., Greco, S., Beltran, T., Lairez, D., Authelin, J. R., and Bazile, D. (2015) A method to Quantify the Affinity of Cabazitaxel for PLA-PEG Nanoparticles and Investigate the Influence of the Nano-Assembly Structure on the Drug/Particle Association. *Pharm. Res.* 32, 1-13.

(12) Bensaid, F., Thillaye, d. B. O., Amgoune, A., Pradel, C., Harivardhan, R. L., Didier, E., Sablé, S., Louit, G., Bazile, D., and Bourissou, D. (2013) Y-shaped mPEG-PLA cabazitaxel conjugates: well-controlled synthesis by organocatalytic approach and self-assembly into interface drug-loaded core-corona nanoparticles. *Biomacromolecules* 14, 1189-1198.

(13) Matsumura, Y., and Maeda, H. (1986) A new concept for macromolecular therapeutics in cancer chemotherapy: mechanism of tumoritropic accumulation of proteins and the antitumor agent smancs. *Cancer Res.* 46, 6387-6392.

(14) Guan, X. (2015) Cancer metastases: challenges and opportunities. *Acta Pharm. Sin. B* 5, 402-418.

(15) Barcellos-Hoff, M. H., Lyden, D., and Wang, T. C. (2013) The evolution of the cancer niche during multistage carcinogenesis. *Nat. Rev. Cancer* 13, 511-518.

(16) Romero-Garcia, S., Lopez-Gonzalez, J. S., B´ ez-Viveros, J. L., Aguilar-Cazares, D., and Prado-Garcia, H. (2011) Tumor cell metabolism: an integral view. *Cancer Biol. Ther.* 12, 939-948.

(17) Mbeunkui, F., and Jr, D. J. J. (2009) Cancer and the tumor microenvironment: a review of an essential relationship. *Cancer Chemother. Pharmacol.* 63, 571-582.

(18) Fukumura, D., and Jain, R. K. (2007) Tumor microenvironment abnormalities: Causes, consequences, and strategies to normalize. *J. Cell. Biochem.* 101, 937-949.

(19) Brülisauer, L., Gauthier, M. A., and Leroux, J. C. (2014) Disulfide-containing parenteral delivery systems and their redox-biological fate. *J. Control. Release* 195C, 147–154.

(20) Yin, T., Wu, Q., Wang, L., Yin, L., Zhou, J., and Huo, M. (2015) Well-Defined Redox-Sensitive Polyethene Glycol–Paclitaxel Prodrug Conjugate for Tumor-Specific Delivery of Paclitaxel Using Octreotide for Tumor Targeting. *Mol. Pharm.* 12, 3020-3031.

(21) Meng, F. H., Zhong, Z. Y., and Feijen, J. (2009) Stimuli-Responsive Polymersomes for Programmed Drug Delivery. *Biomacromolecules* 10, 197-209.

(22) Wang, Y., Liu, D., Zheng, Q., Zhao, Q., Zhang, H., Ma, Y., Fallon, J. K., Fu, Q., Haynes, M. T., and Lin, G. (2014) Disulfide Bond Bridge Insertion Turns Hydrophobic Anticancer Prodrugs into Self-Assembled Nanomedicines. *Nano. Lett.* 14, 5577-5583.

(23) Zhuang, S. R., Chen, S. L., Tsai, J. H., Huang, C. C., Wu, T. C., Liu, W. S., Tseng, H. C., Lee, H. S., Huang, M. C., and Shane, G. T. (2009) Effect of citronellol and the Chinese medical herb complex on cellular immunity of cancer patients receiving chemotherapy/radiotherapy. *Phytother. Res.* 23, 785–790.

(24) Brito, R. G., Guimarães, A. G., Quintans, J. S. S., Santos, M. R. V., Sousa, D. P. D., Badaue-Passos, D., Lucca, W. D., Brito, F. A., Barreto, E. O., and Oliveira, A. P. (2012) Citronellol, a monoterpene alcohol, reduces nociceptive and inflammatory activities in rodents. *J. Nat. Med.* 66, 637-644.

(25) Misra, L. N., Wouatsa, N. A. V., Shiv, K., Kumar, R., Venkatesh, and Francois, T. (2013) Antibacterial, cytotoxic activities and chemical composition of fruits of two Cameroonian Zanthoxylum species. *J. Ethnopharmacol.* 148, 74–80.

(26) Chainani-Wu, N. (2003) Safety and anti-inflammatory activity of curcumin: A component of tumeric (Curcuma longa). *J. Altern. Complement. Med.* 9, 161-168.

(27) Basnet, P., and Skalko-Basnet, N. (2011) Curcumin: An Anti-Inflammatory Molecule from a Curry Spice on the Path to Cancer Treatment. *Molecules* 16, 4567-4598.

(28) Anand, P., Kunnumakkara, A. B., Newman, R. A., and Aggarwal, B. B. (2007) Bioavailability of curcumin: Problems and promises. *Mol. Pharm.* 4, 807-818.

(29) Yuan, F., Dellian, M., Fukumura, D., Leunig, M., Berk, D. A., Torchilin, V. P., and Jain, R. K. (1995) Vascular permeability in a human tumor xenograft: molecular size dependence and cutoff size. *Cancer Res.* 55, 3752-3756.

(30) Feng, L., Michael, D., and Mahato, R. I. (2010) Synthesis and Characterization of Amphiphilic Lipopolymers for Micellar Drug Delivery. *Biomacromolecules* 11, 2610-2620.

(31) Jiang, T., Zhang, Z., Zhang, Y., Lv, H., Zhou, J., Li, C., Hou, L., and Zhang, Q. (2012) Dual-functional liposomes based on pH-responsive cell-penetrating peptide and hyaluronic acid for tumor-targeted anticancer drug delivery. *Biomaterials* 33, 9246–9258.

(32) Rapoport, N. Y., Kennedy, A. M., Shea, J. E., Scaife, C. L., and Nam, K.-H. (2009) Controlled and targeted tumor chemotherapy by ultrasound-activated nanoemulsions/microbubbles. *J. Control. Release* 138, 268-276.

(33) Cristina, F., Sérgio, S. E., and Rogério, G. (2002) Paclitaxel-loaded PLGA nanoparticles: preparation, physicochemical characterization and in vitro anti-tumoral activity. *J. Control. Release* 83, 273–286.

(34) Long, Y., Jian, W., Zhang, D., Aubry, A. F., and Arnold, M. E. (2014) Application of a stabilizer cocktail of N -ethylmaleimide and phenylmethanesulfonyl fluoride to concurrently stabilize the disulfide and ester containing compounds in a plasma LC–MS/MS assay. *J. Pharm. Biomed. Anal.* 88, 552-561.

(35) Zeng, J., Onthank, D., Crane, P., Unger, S., Zheng, N., Pasas-Farmer, S., and Arnold, M. (2007) Simultaneous determination of a selective adenosine 2A agonist, BMS-068645, and its acid metabolite in human plasma by liquid chromatography-tandem mass spectrometry--evaluation of the esterase inhibitor, diisopropyl fluorophosphate, in the stabilization of a labile ester-containing drug. *J. Chromatogr. B* 852, 77-84.

(36) Fung, E. N., Naiyu, Z., Arnold, M. E., and Jianing, Z. (2010) Effective screening approach to select esterase inhibitors used for stabilizing ester-containing prodrugs analyzed by LC-MS/MS. *Bioanalysis* 2, 733-743.

(37) Gund, M., Khanna, A., Dubash, N., Damre, A., Singh, K. S., and Satyam, A. (2015) Water-soluble prodrugs of paclitaxel containing self-immolative disulfide linkers. *Bioorg. Med. Chem. Lett.* 25, 122-127.

(38) Xiuli, H., and Xiabin, J. (2009) Biodegradable amphiphilic polymer-drug conjugate micelles. *Expert Opin. Drug Deliv.* 6, 1079-1090.

(39) Fox, M. E., Guillaudeu, S., Fréchet, J. M., Jerger, K., Macaraeg, N., and Szoka, F. C. (2009) Synthesis and in vivo antitumor efficacy of PEGylated poly(l-lysine) dendrimer-camptothecin conjugates. *Mol. Pharm.* 6, 1562-1572.

(40) Azarenko, O., Smiyun, G., Mah, J., Wilson, L., and Jordan, M. A. (2014) Antiproliferative mechanism of action of the novel taxane cabazitaxel as compared with the parent compound docetaxel in MCF7 breast cancer cells. *Mol. Cancer Ther.* 13, 2092-2103.

(41) Saba, T. M. (1970) Physiology and physiopathology of the reticuloendothelial system. *Arch. Intern. Med.* 126, 1031-1052.

(42) Allen, T. M., and Chonn, A. (1987) Large unilamellar liposomes with low uptake into the reticuloendothelial system. *FEBS Lett.* 223, 42-46.

(43) LiuXiao, T., YueHong, X., Chenyi, T., Lihe, D., and Chuanbin, W. (2012) In vivo imaging in tumor-bearing animals and pharmacokinetics of PEGylated liposomes modified with RGD cyclopeptide. *Acta Pharm. Sin. B* 47, 646-651.

(44) Su, W. P., Cheng, F. Y., Shieh, D. B., Yeh, C. S., and Su, W. C. (2012) PLGA nanoparticles codeliver paclitaxel and Stat3 siRNA to overcome cellular resistance in lung cancer cells. *Int. J. Nanomedicine* 7, 4269–4283.

(45) Tang, B., Fang, G., Gao, Y., Liu, Y., Liu, J., Zou, M., Wang, L., and Cheng, G. (2015) Lipid-albumin nanoassemblies co-loaded with borneol and paclitaxel for intracellular drug delivery to C6 glioma cells with P-gp inhibition and its tumor targeting. *Asian J. Pharm. Sci.* 10, 363-371.

(46) Ma, Y., Liu, D., Wang, D., Wang, Y., Fu, Q., Fallon, J. K., Yang, X., He, Z., and Liu, F. (2014) Combinational Delivery of Hydrophobic and Hydrophilic Anticancer Drugs in Single Nanoemulsions To Treat MDR in Cancer. *Mol. Pharm.* 11, 2623-2630.

884 **Table of Contents Graphic**

885